CircBCBM1 Promotes Breast Cancer Brain Metastasis via miR-125a/BRD4 Axis

Bo Fu
Liaocheng People's Hospital
Wei Liu
Liaocheng People's Hospital
Peng Li
Liaocheng People's Hospital
Li Pan
Liaocheng People's Hospital
Ke Li
Liaocheng People's Hospital
Peiying Cai
Liaocheng People's Hospital
Min Meng
Liaocheng People's Hospital
Yiting Wang
Liaocheng People's Hospital
Anqi Zhang
Liaocheng People's Hospital
Wenqiang Tang
Liaocheng People's Hospital
Meng An (anm@lchospital.cn)
Liaocheng People's Hospital

Research

Keywords: breast cancer brain metastasis, circBCBM1, miR-125a, BRD4, biomarker, therapeutic target

Posted Date: December 22nd, 2020

DOI: https://doi.org/10.21203/rs.3.rs-130879/v1

Abstract

Background: Accumulating evidence indicates that circular RNAs (circRNAs) play critical roles in tumorigenesis and progression of various cancers. We previously identified a novel upregulated circRNA, circBCBM1 (hsa_circ_0001944), in the context of breast cancer brain metastasis. However, the potential biological function and molecular mechanism of circBCBM1 in breast cancer brain metastasis remain largely unknown.

Methods: In this reserch, we validated the expression and characterization of circBCBM1 through RT-qPCR, Sanger sequencing, RNase R assay and fluorescence in situ hybridization (FISH). Functional experiments were performed to determine the effect of circBCBM1 on growth and metastasis of 231-BR cells both *in vitro* and *in vivo*. The regulatory mechanisms among circBCBM1, miR-125a (has-miR-125a-5p), and BRD4 (bromodomain containing 4) were investigated by RNA immunoprecipitation (RIP), RNA pull-down, luciferase reporter assay and western blot.

Results: Our findings demonstrated that circBCBM1 is a stable and cytoplasmic circRNA. Functionally, silencing of circBCBM1 led to decreased proliferation and migration of 231-BR cells whereas elevated circBCBM1 expression showed reverse effects *in vitro*. These findings were confirmed *in vivo* in mouse models, as knockdown of circBCBM1 significantly decreased growth and brain metastases of 231-BR cells. Mechanistically, circBCBM1 functions as an endogenous miR-125a sponge to inhibit miR-125a activity, resulting in the upregulation of BRD4 expression and subsequent upregulation of MMP9 (matrix metallopeptidase 9) through Sonic hedgehog (SHH) signaling pathway. Importantly, circBCBM1 was markedly upregulated in the breast cancer brain metastasis cells and clinical tissue and plasma samples; besides, the overexpression of circBCBM1 in primary cancerous tissues was associated with shorter brain metastasis-free survival (BMFS) of breast cancer patients.

Conclusions: These findings indicate that circBCBM1 is involved in breast cancer brain metastasis via circBCBM1/miR-125a/BRD4 axis, which sheds light on the pathogenic mechanism of circBCBM1 and provides translational evidence that circBCBM1 may serve as a novel diagnostic or prognostic biomarker and potential therapeutic target for breast cancer brain metastasis.

Introduction

Brain metastases represent the most common intracranial neoplasm in adults and breast cancer is the second most common cause of brain metastases [1, 2]. Approximately 10–30% of breast cancer patients will develop brain metastases [3]. Breast cancer brain metastasis is becoming an increasingly common diagnosis due to improved systemic therapy and more routine imaging surveillance [4]. Breast cancer brain metastases often induce neurological impairments by affecting cognitive and sensory functions and confer a poor prognosis, with an approximately 80% mortality within one year after diagnosis [5]. The initiation and progression of brain metastases are staged into primary tumor cells' invasion, intravasation, dissemination, extravasation and colonization [6]. However, the biological mechanism

underlying establishment and progression of breast cancer brain metastasis remains largely unknown. Identification of the cellular and molecular mechanisms underlying breast cancer brain metastasis is desperately needed to provide a basis for the development of innovative diagnostic biomarkers and therapeutic targets.

Circular RNAs (circRNAs) are emerging subgroup of endogenous noncoding RNAs. CircRNAs are single-stranded, covalently closed RNA molecules that are generated by back-splicing of precursor mRNAs [7]. CircRNAs are characterized by a stable loop structure, evolutionary conservation, and high cell type-, tissue- or developmental stage-specific expression [8]. Compare with linear counterparts, circRNAs are more stable because they lack accessible ends and are thus resistant to exonuclease-mediated digestion [9]. CircRNAs have well-learned functions include sequestration of microRNAs (miRNAs) or proteins, modulation of RNA polymerase II (Pol II) transcription and interference with pre-mRNA splicing, and even translation to produce peptides, while the biological function of most circRNAs remains largely unexplored [10]. Aberrant expression of circRNAs was found implicated in various cancers, including hepatocellular carcinoma [11, 12], gastric cancer [13], oral squamous cell carcinoma [14], lung adenocarcinoma [15], colorectal cancer [16], etc.

In our previous study, we primarily revealed the circRNA profile related to breast cancer brain metastases and identified 406 differentially expressed circRNAs between the brain metastatic 231-BR cells and the parental nonspecific metastatic MDA-MB-231 cells [17]. Among these circRNAs, has_circ_0001944 (termed as circBCBM1 for brief) was one of the most significantly upregulated molecules in breast cancer brain metastases. As a novel circRNA, its biological function and molecular mechanism in breast cancer brain metastasis await elucidation. In this study, we found that in the context of breast cancer brain metastasis, circBCBM1 dramatically promoted cell proliferation and migration of 231-BR cells. Further study revealed that circBCBM1 could function as a sponge of has-miR-125a-5p (abbreviated as miR-125a) to upregulate bromodomain containing 4 (BRD4) and then upregulate matrix metallopeptidase 9 (MMP9) through Sonic hedgehog (SHH) signaling pathway, and consequently promote brain metastatic breast cancer cells' migration *in vitro* and metastasis *in vivo*. Moreover, circBCBM1 was upregulated in the breast cancer brain metastasis cells and clinical tissue and plasma samples, and the overexpression of circBCBM1 in primary cancerous tissues was correlated with shorter brain metastasis-free survival (BMFS) of breast cancer patients. Therefore, circBCBM1 may act as an oncogene to promote breast cancer brain metastasis and may serve as a potential diagnostic or prognostic biomarker and therapeutic target for breast cancer brain metastasis.

Materials And Methods

Clinical samples

In total, 13 pairs of breast cancer (BC) and adjacent normal breast tissues (NBT) (cohort 1), 6 breast cancer brain metastasis (BCBM) tissues (cohort 2), 20 BC and 20 BCBM patients' plasma samples (cohort 3), and 53 BCBM patients' primary tumor tissues (cohort 4) were collected from Liaocheng

People's Hospital (Liaocheng, China). CircBCBM1 expression at the tissue level was quantified in cohort 1 and 2, that at the plasma level was quantified in cohort 3, and Kaplan-Meier analysis of the correlation between circBCBM1 expression and BMFS was conducted with data of cohort 4. Specimens were identified by two pathologists independently. Clinical information of the enrolled patients was collected from their electronic medical records. Informed consents were obtained from all participants. The study was approved by the Ethics Committee of Liaocheng People's Hospital.

Cell culture

Human brain-targeting breast carcinoma cell line 231-BR and its parental cell line MDA-MB-231 were kindly provided by Patricia S Steeg (National Cancer Institute, NIH, Bethesda, MD, USA). Breast cancer cell line BT-474 and T47D were purchased from American Type Culture Collection (ATCC; Manassas, VA, USA). All cells were cultured in Dulbecco's Modified Eagle Medium (DMEM; Invitrogen, CA, USA) supplemented with 10% (v/v) fetal bovine serum (FBS; Gibco, Vienna, Austria) with 5% CO2 at 37 °C.

RNA preparation and real-time quantitative PCR (RT-qPCR) analysis

For RNase R treatment, total RNA (2 μg) was incubated with or without RNase R (3 U/μg; Epicentre Technologies, Madison, WI, USA) in 1×RNase R reaction buffer for 20 min at 37 °C, and the resulting RNA was purified using an RNeasy MinElute cleanup Kit (Qiagen). For cellular RNA fractionation analysis, the cells' nuclear and cytoplasmic fractions were extracted using NE-PER Nuclear and Cytoplasmic Extraction Reagents (Thermo Scientific). The total RNA was extracted using TRIzol reagent (Invitrogen, CA, USA).

For circBCBM1 and BRD4 detection, the cDNAs were synthesized using PrimeScript RT Master Mix (Takara, Dalian, China) according to the manufacturer's instructions. The RT-qPCR was performed using TG Green Premix Ex Taq II kit (Takara, Dalian, China) with a 7500 Real-Time PCR System (Applied Biosystems, Foster City, CA) as previously described [18]. *GAPDH* served as an internal reference gene. For miR-125a detection, the cDNAs were synthesized using miRNA First Strand cDNA Synthesis kit (Stem-loop Method; Shanghai Sangon Biotech, Shanghai, China) according to the manufacturer's instructions. Then qPCR was performed using MicroRNAs qPCR Kit (SYBR Green Method; Shanghai Sangon Biotech, Shanghai, China). *U6* served as an internal reference gene. All primer sequences are listed in Supplementary Table S1.

RNA fluorescence in situ hybridization (FISH)

Cy3-labelled circBCBM1 FISH mix probe was designed and synthesized by Guangzhou RiboBio Co., Ltd. (Guangzhou, China). FISH was conducted using Ribo Fluorescent In Situ Hybridization Kit (RiboBio, Guangzhou, China). Briefly, 231-BR cells (60-70% confluent) were fixed, permeated and hybridized with circBCBM1 probe at 37 °C overnight. The hybridization buffer was then gradually eluted with 4× saline-sodium citrate (SSC), 2× SSC and 1× SSC. Nuclei were counterstained with 4,6-diamidino-2-phenylindole (DAPI). 18S and U6 served as reference probes. The images were acquired on a Leica SP5 confocal microscope (Leica Micosystems, Mannheim, Germany).

Oligonucleotides, plasmids and transfection

siRNA, miRNA mimics and inhibitors were designed and synthesized by RiboBio (Guangzhou, China) or Sangon Biotech (Shanghai, China). Transfection was performed using Lipofectamine 2000 reagent (Invitrogen, Carlsbad, USA) or riboFECT CP transfection kit (RiboBio, Shanghai, China). The overexpressing and silencing vectors were constructed by HANBIO (Shanghai, China) as described previously [19]. All constructs were verified by sequencing. Lentiviral particles carrying the above-mentioned vectors were generated in HEK293T cells. 231-BR cells were infected with lentivirus at a multiplicity of infection (MOI) of 30, and screened by puromycin.

Cell counting kit-8 (CCK8) and colony formation assays

For CCK8 assay, cells were seeded into 96-well plates and cultured overnight, followed by gene silencing or overexpression treatment. After culture, CCK8 (10 μL; Dojindo, Japan) solution was added to each well and incubation for 2 h. Absorbance at 450 nm was measured using microplate reader (BioTex, Houston, TX, USA). For colony formation assay, cells were seeded into 6-well plates with 1×10^3 cells/well. After 14 days of culture, cells were fixed with 4% (w/v) paraformaldehyde (PFA) and stained with 0.1% crystal violet.

Apoptosis detection assay

Apoptosis detection assay was conducted using PE Annexin V Apoptosis Detection Kit I (BD Pharmingen, Franklin Lakes, NJ, USA) according to the manufacturer's procedure. Briefly, cells were harvested, washed and resuspended in 1 × binding buffer, and incubated with 5 μL PE Annexin V and 5 μL 7-AAD for 15 min. The apoptotic cells were assessed using a FACSCalibur flow cytometer (BD Bioscience, San Jose, CA, USA).

Wound healing and transwell migration assays

For wound healing assay, cells were seeded into a 6-well plate and scraped using a pipette tip. Images were obtained using an inverted light microscope at the time points of 0 and 24 h. For transwell migration assay, cells were seeded into the upper chamber. After incubation, the cells were fixed with methanol and stained with crystal violet. Then, the non-migrated cells that remained at the top layer were removed using a cotton swab and migrated cells at the bottom of the chamber were observed and counted under a light microscope.

Animal models

Six-week-old female BALB/c nu/nu mice were obtained from Beijing Vital River Laboratory Animal Technology (Beijing, China). The subcutaneous tumor model was generated by subcutaneously injection (s.c) of 231-BR cells (5×10^6) into the right shoulder of the mouse. The breast cancer brain metastasis model was generated by injecting 231-BR cells (2×10^5 cells in 0.1 ml PBS) into the left ventricle of the mouse heart. Mice were euthanized after four weeks. Mouse brains were collected and stained with

hematoxylin and eosin (H&E) as previously described for metastatic nodules count [20]. All animal experiments were conducted in accordance with the protocols evaluated and approved by the Institutional Animal Care and Use Committee of Liaocheng People's Hospital.

RNA immunoprecipitation (RIP) assay

RIP assay was conducted using EZ-Magna RIP RNA-Binding Protein Immunoprecipitation Kit (Millipore, Billerica, MA, USA) according to the manufacturer's protocol. Cells were lysed in 100 μl RIP lysis buffer and then diluted with 900 μl RIP immunoprecipitation buffer. The cell suspension was then mixed with magnetic beads conjugated with anti-Argonaute 2 (Ago2) or control anti-IgG antibody and rotated overnight at 4°C. The beads were collected and washed using RIP washing buffer and treated with Proteinase K at 55 °C for 30 min. RNA was extracted using TRIzol reagent (Invitrogen, CA, USA) and analyzed by RT-qPCR.

Biotinylated RNA pull-down assay

The biotinylated RNA pull-down assay was performed as described previously [19]. The 3′-biotinylated miRNA and circRNA probes were designed and synthesized by RiboBio (Guangzhou, China) or GenePharma (Shanghai, China). To pull down circRNA by miRNA, 231-BR cells were transfected with biotinylated miR-125a, miR-1306, miR-34c, miR-26a, miR-10399, miR-661 or control miRNA. 48 h later, the cells were washed and lysed on ice for 10 min. Lysates were incubated with Dynabeads™ M-280 Streptavidin magnetic beads (Invitrogen, 11205D) at 4°C for 1.5 h. The bound RNAs were purified using TRIzol for RT-qPCR analysis. To pull down miRNA by circRNA, the biotinylated circBCBM1 probe was incubated with M-280 Streptavidin magnetic beads (Invitrogen, 11205D) at 4°C for 3 h to generate probe-coated magnetic beads. 231-BR cells were lysed and incubated with probe-coated beads at 4 °C overnight. After washing, the bound RNAs were extracted for RT-qPCR analysis.

Luciferase reporter assay

HEK293T cells were seeded in a 96-well plate and cultured for 24 h. The cells were co-transfected with a mixture of miRNA mimics (5 pmol) and luciferase reporter vectors (pSI-Check2) containing BRD4 3'-UTR sequences (0.16 μg), alongside with a negative control miRNA, to examine the miRNA binding ability. After 48 h, the luciferase activity was determined using a dual luciferase reporter assay system (Promega, Madison, WI, USA) following the manufacturer's protocol. Renilla luciferase activity was normalized to firefly luciferase activity and expressed as the percentage of the control.

Western blotting analysis

Proteins were extracted in RIPA lysis buffer (P0013B, Beyotime) and the concentration was determined using BCA Protein assay kit (P0010S, Beyotime). Proteins were separated on sodium dodecyl sulfate-polyacrylamide gels and then transferred to polyvinylidene fluoride (PVDF) membranes. The membranes were blocked with 5% non-fat dry milk and then incubated overnight with primary antibodies, including anti-BRD4 (ab128874, Abcam), anti-MMP9 (ab38898, Abcam), anti-Shh (2207s, CST), anti-Gli1 (2643s,

CST) and anti-GAPDH (sc-32233, Santa Cruz Biotechnology). Membranes were then incubated with horseradish peroxidase (HRP)-conjugated goat anti-mouse/rabbit IgG secondary antibody at room temperature. The blots were detected by chemiluminescence and imaged on an AlphaView analysis system (ProteinSimle, USA). The quantification of individual protein bands was assessed by densitometry using ImageJ software.

mRNA sequencing

Total RNA from 231-BR cells or MDA-MB-231 cells was extracted using TRIzol reagent (Invitrogen, CA, USA). Ribosomal RNA was removed by Epicentre Ribo-zero rRNA Removal Kit (Epicentre, USA). The sequencing libraries were generated by NEBNext Ultra Directional RNA Library Prep Kit (NEB, Beverly, USA) following the manufacturer's protocol. Briefly, RNA was fragmented and first-strand cDNA was synthesized using random hexamer primers and M-MuLV ReverseTranscriptase (RNaseH-). The second strand cDNA synthesis was performed using DNA Polymerase I and RNase H, with dUTP replacing dTTP in the reaction buffer. After adenylation at the 3' ends of cDNA fragments, NEBNext Adaptor with a hairpin loop structure was ligated for hybridization. The library fragments were purified with AMPure XP system (Beckman Coulter, Beverly, US) and then treated by 3 μL USER Enzyme (NEB, Beverly, USA) at 37 °C for 15 min followed by 95 °C for 5 min. After PCR amplification, the products were purified and library quality was assessed on Agilent Bioanalyzer 2100 (Agilent Technologies, CA, USA). The index-coded library was clustered on cBot Cluster Generation System (Illumina Inc., San Diego, CA), and was sequenced on Illumina HiSeq 2500 platform and 125 bp paired-end reads were generated. An index of the reference genome was built and paired-end clean reads were mapped to the reference genome using HISAT2. The mapped reads of each sample were assembled by StringTie. Differential expression of replicated count data was examined using edgeR software package.

Statistical analysis

All *in vitro* experiments were repeated at least three times. The quantitative data were expressed as means ± standard error of the mean (SEM) and analyzed by *t* test or one-way ANOVA. BMFS was defined as the time from the date of surgery to the date of brain metastasis. BMFS was calculated with Kaplan-Meier estimates and analyzed with the log-rank test. All statistical analyses were performed using SPSS18 software (SPSS Inc., Chicago, USA). $P < 0.05$ was considered statistically significant.

Results

Characterization of circBCBM1 in 231-BR cells

We previously identified the circRNA expression profile of brain metastatic breast cancer cell line 231-BR, in comparison with its parental nonspecific metastatic cell line MDA-MB-231, using RNA-seq [17]. CircBCBM1 was one of the most significantly upregulated circRNAs in 231-BR cells. CircBCBM1 is derived from a long non-coding RNA region within the FIRRE locus (chrX:130883333–130928494), which is located on chromosome Xq26.2. The distinct product of expected size was amplified by outward-facing

primers and was confirmed by Sanger sequencing (Fig. 1A). Its resistance to RNase R exonuclease digestion further confirmed that it exists in a circular form (Fig. 1B).

We next sought to investigate the stability and localization of circBCBM1. After treatment with transcription inhibitor Actinomycin D, the expression level of the circular RNA isoform of circBCBM1 remained stable, while its linear counterpart level was remarkably decreased (Fig. 1C). Cellular RNA fractionation analysis showed that circBCBM1 was predominately localized within cytoplasm instead of nuclei in 231-BR cells ($P = 0.003$; Fig. 1D). FISH result further confirmed circBCBM1's distribution (Fig. 1E). Taken together, the results implied that circBCBM1 is a stable and cytoplasmic circRNA.

CircBCBM1 promotes proliferation and migration of 231-BR cells in vitro

To evaluate the biological functions of circBCBM1, we designed a specific siRNA oligonucleotide to target the unique backsplice junction. A nonspecific siRNA sequence served as control. As expected, the backsplice junction-specific siRNA inhibited circBCBM1 expression but did not affect the linear counterpart level (Fig. 2A). CCK8 assay showed that the downregulation of circBCBM1 significantly suppressed 231-BR cell proliferation ($P = 0.025$; Fig. 2B). Colony formation assay showed that circBCBM1 silencing significantly inhibited colony-forming of 231-BR cells ($P = 0.047$; Fig. 2C). Annexin V-PE/ 7-AAD staining demonstrated that circBCBM1 silencing significantly promoted cellular apoptosis ($P = 0.003$; Fig. 2D). Wound healing and transwell migration experiments revealed that circBCBM1 silencing significantly inhibited migration of 231-BR cells ($P < 0.05$; Fig. 2E and 2F).

To further verify the role of circBCBM1, circBCBM1-overexpressing 231-BR cells were constructed by transfecting expression plasmids for circBCBM1. As shown in Supplementary Figure S1A, the relative expression level of the circular RNA isoform of circBCBM1 was dramatically increased ($P = 0.032$), while its linear counterpart did not increase significantly ($P = 0.388$). Cell viability was prominently increased after circBCBM1 transfection ($P = 0.006$; Supplementary Figure S1B), as well as cell migration capability ($P = 0.001$; Supplementary Figure S1C). Collectively, these findings indicate that circBCBM1 promotes cell proliferation and migration of 231-BR cells *in vitro*.

CircBCBM1 facilitates growth and brain metastasis of 231-BR cells in vivo

Based on our *in vitro* findings that circBCBM1 was involved in cell proliferation and migration of 231-BR cells, we further explored the role of circBCBM1 in tumor growth and brain metastasis *in vivo*. Tumor growth was researched by subcutaneous injecting 231-BR cells with circBCBM1 stable knockdown (sh-circBCBM1) into nude mice, and we found that circBCBM1 knockdown significantly decreased tumor volumes and weights (Fig. 3A-3D).

Brain metastasis was explored by injecting 231-BR cells with circBCBM1 stable knockdown (sh-circBCBM1) into the left cardiac ventricle of nude mice. Four weeks after injection, the mouse brains were excised for hematoxylin and eosin (H&E) staining. The total count of brain metastasis nodules was found significantly decreased in the sh-circBCBM1 group compared with that in the control group ($P = 0.002$;

Fig. 3E). We further categorized the metastasis nodules into large (> 50 μm^2) and micro-metastases (≤ 50 μm^2) (Fig. 3F). Compared with the control group, the counts of large metastases and micro-metastases in the sh-circBCBM1 group were both significantly decreased (P = 0.019 and 0.001, respectively; Fig. 3G).

We also assessed the effect of circBCBM1 stable overexpressing on brain metastasis of 231-BR cells. As shown in Supplementary Figure S2A and S2B, both large metastases and micro-metastases in the circBCBM1-overexpressing group were evidently increased relative to that in the control group (P = 0.026 and 0.006, respectively). Collectively, these findings demonstrate that circBCBM1 facilitates tumor growth and brain metastasis of 231-BR cells *in vivo.*

Circbcbm1 Serves As A Sponge For Mir-125a

Having determined the essential role of circBCBM1 in the context of breast cancer brain metastasis, we tried to get insight into the mechanisms of circBCBM1 regulation. Given that circRNAs can act as competing endogenous RNA sponges to interact with miRNAs and influence their activity, we explored whether circBCBM1 functions as a miRNA sponge in 231-BR cells by conducting RNA RIP assay with Ago2 antibody. As shown in Fig. 4A, endogenous circBCBM1 was significantly enriched by anti-Ago2 compared with the control IgG antibody (P = 0.031), suggesting that circBCBM1 is able to bind to Ago2 and miRNAs.

To dissect which miRNA circBCBM1 binds to, we conducted bioinformatics analysis using miRanda and identified 6 candidate miRNAs, including miR-125a, miR-1306, miR-34c, miR-26a, miR-10399 and miR-661 (Supplementary Table S2). In miRNA pull-down assay using biotin-coupled miRNA mimics, circBCBM1 was only efficiently enriched by miR-125a, but not by the other five miRNAs (Fig. 4B). In RIP assay, miR-125a was efficiently pulled down by anti-Ago2 antibody (Fig. 4C). An inverse affinity isolation assay using a biotin-labeled specific circBCBM1 probe also confirmed that circBCBM1 probe, but not the random probe, bound to miR-125a (Fig. 4D). Compared with the siRNA control, silencing of circBCBM1 significantly decreased the miR-125a levels in 231-BR cells (Fig. 4E). In the parental MDA-MB-231 cells, the relative miR-125a level was significantly higher than 231-BR cells (Fig. 4F). Collectively, these findings provide evidence that circBCBM1 acts as a sponge for miR-125a in 231-BR cells.

Brd4 Is The Downstream Target Of Mir-125a

To elucidate the molecular mechanisms by which circBCBM1/miR-125a involved in breast cancer brain metastasis, we identified a potential target gene, *BRD4*, using TargetScan, which has a potential miR-125a binding site within its 3′-UTR (Fig. 5A). We next cloned the wild-type and mutant (with mutated predicted miR-125a binding site) 3'-UTR of *BRD4* mRNA and performed dual-luciferase reporter assay. As shown in Fig. 5B, 231-BR cells co-transfected with miR-125a mimic and pmiR-GLO plasmid with wild-type BRD4 3′-UTR showed down-regulated luciferase activity (P = 0.001), whereas this effect was not

observed in the mutated BRD4 3′-UTR. The result suggested that the predicted binding element was essential for miR-125a binding to the 3'-UTR of BRD4.

In the comparison between 231-BR cells and MDA-MB-231 cells, gene expression profile showed that *BRD4* was significantly increased in 231-BR cells (BCBM group) (Fig. 5C), which was further confirmed at both mRNA ($P = 0.011$; Fig. 5D) and protein levels ($P = 0.037$; Fig. 5E). Moreover, in 231-BR cells, miR-125a mimics reduced BRD4 expression ($P = 0.024$; Fig. 5F), whereas miR-125a inhibitors improved BRD4 expression at the protein level ($P = 0.040$; Fig. 5G). Taken together, these findings reveal that miR-125a bind to 3'-UTR of BRD4 and directly downregulate its expression.

Circbcbm1 Promotes Cell Migration Via Circbcbm1/mir-125a/brd4 Axis

Having determined that BRD4 is the downstream target of miR-125a, we hypothesized that circBCBM1 promotes cell migration via circBCBM1/miR-125a/BRD4 axis. Firstly, we examined the effect of circBCBM1 on BRD4 expression. As shown in Fig. 6A and 6B, circBCBM1 silencing decreased the expression of BRD4 at both mRNA ($P = 0.019$) and protein level ($P = 0.037$). On the contrary, circBCBM1 overexpression increased the protein level of BRD4 ($P = 0.016$; Fig. 6C).

To further verify that miR-125a acts as a mediator of circBCBM1 to control the expression of BRD4, we conducted rescue experiments. Overexpression of circBCBM1 significantly lessened the decreased expression of BRD4 induced by miR-125a mimics in 231-BR cells ($P < 0.001$; Fig. 6D). Moreover, knockdown of circBCBM1 attenuated the inductive effects of miR-125a inhibitors on the expression of BRD4 ($P < 0.001$; Fig. 6E). More importantly, transwell migration experiments showed that miR-125a mimics abolished the enforced cell migration induced by circBCBM1 (Fig. 6F). Collectively, these findings suggest that circBCBM1 promotes 231-BR cells' migration via circBCBM1/miR-125a/BRD4 axis.

BRD4 promotes MMP9 expression through SHH signaling pathway in 231-BR cells

Previously studies found that MMP9 contributed to breast cancer brain metastasis through promoting cells' trans-endothelial migration and permeability across blood-brain barrier (BBB), and its expression level was correlated with breast cancer brain metastasis-free survival [21–24]. We next sought to examine the effect of BRD4 expression on MMP9 level in 231-BR cells. As shown in Fig. 7A and 7B, BRD4 silencing resulted in decreased MMP9 expression ($P = 0.004$), while BRD4 overexpression led to increased MMP9 expression ($P = 0.001$). Mechanistically, a previous study demonstrated that BRD4 regulated MMP-9 expression through the SHH signaling pathway in hepatocellular carcinoma cells [25]. In the context of breast cancer brain metastasis in our study, we also found BRD4 silencing caused downregulation of downstream target molecule Shh and Gli, while BRD4 overexpression improved the two target molecules' expression (Fig. 7A and 7B), suggesting that BRD4 may promote MMP9 expression through SHH signaling pathway in 231-BR cells.

CircBCBM1 may act as a potential diagnostic and prognostic biomarker

Considering the vital role and underlying mechanism of circBCBM1 in breast cancer brain metastasis, we hypothesized that circBCBM1 could be used as a diagnostic or prognostic biomarker. We examined the expression levels of circBCBM1 in various breast cancer cell lines and found circBCBM1 was significantly upregulated in brain metastatic 231-BR cells compared with the other cell lines (MDA-MB-231, BT-474 and T47D) ($P < 0.001$; Fig. 8A). We also examined the expression level of circBCBM1 in tissue samples, which showed that circBCBM1 was markedly upregulated in breast cancer brain metastasis tissues compared with other breast cancer and normal breast tissues ($P = 0.044$ and 0.002, respectively; Fig. 8B). Given that blood is the most common sample and liquid biopsy is a less invasive laboratory technique [26], we attempted to figure out the circBCBM1 level in plasma of breast cancer patients with or without brain metastases. By RT-qPCR, we found circBCBM1 was detectable in plasma samples. In agreement with the results from tissue samples, circBCBM1 level was significantly higher in brain metastasis patients' plasma than those in patients without metastases ($P = 0.002$; Fig. 8C), indicating its translational potential as a biomarker for breast cancer brain metastasis patient identification.

To evaluate whether circBCBM1 could serve as a prognostic marker, BMFS curve was plotted by Kaplan-Meier estimates according to the circBCBM1 expression level in their primary site counterparts. As shown in Fig. 8D, breast cancer patients with high expression level of circBCBM1 had significantly shorter BMFS (24 months *vs* 64 months, $P < 0.001$), suggesting that the circBCBM1 level in primary tumor tissue may act as a potential biomarker for predicting the risk of brain metastasis in breast cancer patients.

Discussion

Brain metastasis is a fatal neurological complication accompanying systemic cancers. Identification of key molecules and mechanisms in breast cancer brain metastasis is a prerequisite for the development of diagnostic or prognostic biomarkers and therapeutic targets for future innovative treatments. In this study, we elucidated a novel mechanism that breast cancer brain metastasis may be regulated by circBCBM1/miR-125a/BRD4 signaling axis. We found upregulation of circBCBM1 stimulated 231-BR cell proliferation and migration *in vitro* and growth and brain metastasis *in vivo*. Moreover, circBCBM1 was upregulated in brain metastatic breast cancer cells, clinical patients' tissue and plasma samples, and high circBCBM1 level was associated with short BMFS. To the best of our knowledge, this is the first report that thoroughly investigated the expression, function and molecular mechanism of circBCBM1 in human breast cancer brain metastasis.

CircRNAs belong to a novel class of ncRNAs that have attracted numerous research attention. Mounting evidence demonstrates that circRNAs play an important role in tumorigenesis and progression [27]. Our findings revealed that circBCBM1 was upregulated in the breast cancer brain metastasis tissues, and the high expression level of circBCBM1 in primary cancerous tissues was correlated with short BMFS, suggesting that circBCBM1 may serve as a potential biomarker for predicting the risk of brain metastasis in breast cancer patients. CircRNAs are more stable than their linear counterparts due to their covalent

closed cyclic structure and therefore are enriched in plasma, cell-free saliva, and even in circulating exosomes, which may predict the occurrence of cancer and other diseases [7, 28]. In the present study, we found circBCBM1 was detectable in plasma samples, and its expression level was significantly increased in breast cancer brain metastasis patients' plasma than those in patients without metastases, suggesting that circBCBM1 may serve as a potential circulating biomarker for distinguishing breast cancer patients with brain metastases from those patients without metastases.

Apart from acting as diagnostic or prognostic biomarkers, circRNAs may also be developed into therapeutic targets [29, 30]. Huang et al. reported that specific blockage of circHIPK2 could be a potential therapeutic target for inhibition of astrocyte activation in the context of drug abuse as well as the treatment of a broad range of neuroinflammatory disorders [31]. Yang et al. found that circPTK2 exerts a critical role in the growth and metastasis of colorectal cancer (CRC) and may serve as a therapeutic target for CRC metastasis [16]. Our findings showed circBCBM1 upregulation facilitates 231-BR cell proliferation and migration *in vitro* and growth and brain metastasis *in vivo*, whereas circBCBM1 silencing has reverse effects. These results suggested that circBCBM1 may act as an oncogene, and could be envisioned as a novel therapeutic target for breast cancer brain metastasis.

Based on accumulating evidence, the most explored function of circRNAs is regulating gene expression through ´sponge´ other gene expression regulators, in particular miRNA [32]. For example, circPTCH1 could act as sponge for miR-485-5p to promote invasion and metastasis in renal cell carcinoma [33]. Hsa_circ_0000326 interacted with miR-338-3p to facilitate lung adenocarcinoma progression [34]. Herein, we predicted and verified that circBCBM1 contained a direct binding site of miR-125a, which suggested that circBCBM1 might serve as a miR-125a sponge to promote proliferation and migration of 231-BR cells. Recent studies have shown that circRNAs also functions as scaffolding protein or translational templates [35]. Further investigation is still required to elucidate whether circBCBM1 is involved in these biological processes.

MiRNAs are a class of non-coding small RNAs that post-transcriptionally regulate gene expression by binding to specific mRNA targets and promoting mRNA degradation and/or inhibiting mRNA translation [36]. Recently, miR-125a has been reported as a tumor suppressor that was significantly downregulated in multiple cancer types, such as non-small cell lung cancer [37], gastric cancer [38], bladder cancer [39], etc. In our study, BRD4 was predicted as the candidate target gene of miR-125a by Targetscan and was verified by dual luciferase reporter assay. Our rescue experiments further revealed that circBCBM1 promotes 231-BR cells' migration via circBCBM1/miR-125a/BRD4 axis.

BRD4, a member of the bromodomain and extra-terminal (BET) family, is a crucial epigenetic regulator. Multiple studies reported that BRD4 elevated oncogenic protein level and accelerated carcinogenesis and progression [40, 41]. Wang et al. reported that BRD4 regulated MMP-9 expression through SHH signaling pathway in hepatocellular carcinoma cells [25]. Consistent with this finding, our data showed BRD4 regulated MMP-9 expression and key signaling molecules of SHH pathway. Taken together with the previous report that MMP9 expression was strongly correlated with BMFS of breast cancer patients [24],

we hypothesis that BRD4's function in breast cancer brain metastasis relies on upregulating MMP9 expression via SHH signaling pathway, while the exact mechanism requires further investigation.

Conclusions

Our study revealed that circBCBM1 promoted 231-BR cell proliferation and migration *in vitro* and growth and brain metastasis *in vivo*. Mechanistically, circBCBM1 increased BRD4 expression via acting as miR-125a sponge. Importantly, circBCBM1 was upregulated in brain metastasis patients' tissue and plasma samples, and the high expression level of circBCBM1 in primary cancerous tissues was associated with short BMFS. Taken together, our study clarified that circBCBM1 accelerated breast cancer brain metastasis via circBCBM1/miR-125a/BRD4 axis, and provided innovative candidate targets for breast cancer brain metastasis diagnosis and therapy.

Abbreviations

circRNAs, circular RNAs; miRNAs, microRNAs; Pol II, RNA polymerase II; BMFS, brain metastasis-free survival; BRD4, bromodomain containing 4; MMP9, matrix metallopeptidase 9; SHH, Sonic hedgehog; BC, breast cancer; NBT, adjacent normal breast tissues; BCBM, breast cancer brain metastasis; ATCC, American Type Culture Collection; DMEM, dulbecco's modified eagle medium; FBS, fetal bovine serum; RT-qPCR, real-time quantitative PCR; FISH, fluorescence in situ hybridization; DAPI, 4,6-diamidino-2-phenylindole; MOI, multiplicity of infection; CCK8, cell counting kit-8; PFA, paraformaldehyde; H&E staining, hematoxylin and eosin staining; RIP, RNA immunoprecipitation; Ago2, Argonaute 2; PVDF, polyvinylidene fluoride; HRP, horseradish peroxidase; SEM, standard error of the mean; CRC, colorectal cancer; BET, bromodomain and extra-terminal.

Declarations

Ethics approval and consent to participate

All clinical tissue and plasma samples were collected from Liaocheng People's Hospital under the approval by the Ethics Committee of Liaocheng People's Hospital. Informed consents were obtained from all participants. All animal experiments were conducted in accordance with the protocols evaluated and approved by the Institutional Animal Care and Use Committee of Liaocheng People's Hospital.

Consent for publication

Not applicable.

Availability of data and material

The datasets used and/or analysed during the current study are available from the corresponding author on reasonable request.

Competing interests

The authors declare that they have no competing interests

Funding

This work was supported by funding from the National Natural Science Foundation of China (No. 81702884), Medicine and Health Science Technology Foundation of Shandong Province (No. 2015WS0381 and No. 2016WS0216) and Science Foundation of Liaocheng People's Hospital (No. LYQN201901 and No. LYQN201902)

Authors' contributions

BF, WL, LP, KL, PYC, MM, YTW, AQZ, WQT and MA performed the experiments and analyses. PL and MA collected the samples from patients and contributed to data acquisition. MA, AQZ, WQT and BF conceived and designed the study and experiments. BF, AQZ and MA wrote and edited the paper. All authors contributed to this manuscript. All authors read and approved the final manuscript.

Acknowledgements

Not applicable.

References

1. Salomon MP, Orozco JIJ, Wilmott JS, Hothi P, Manughian-Peter AO, Cobbs CS, Scolyer RA, Hoon DSB, Marzese DM. Brain metastasis DNA methylomes, a novel resource for the identification of biological and clinical features. Sci Data. 2018;5:180245.
2. Abu-Khalaf M, Muralikrishnan S, Hatzis C, Canchi D, Yu JB, Chiang V. Breast cancer patients with brain metastasis undergoing GKRS. Breast Cancer. 2019;26:147–53.
3. Hosonaga M, Saya H, Arima Y. Molecular and cellular mechanisms underlying brain metastasis of breast cancer. Cancer Metastasis Rev. 2020.
4. Mills MN, Figura NB, Arrington JA, Yu H-HM, Etame AB, Vogelbaum MA, Soliman H, Czerniecki BJ, Forsyth PA, Han HS, Ahmed KA. Management of brain metastases in breast cancer: a review of current practices and emerging treatments. Breast cancer research treatment. 2020. 10.1007/s10549-10020-05552-10542.
5. Lowery FJ, Yu D. Brain metastasis: Unique challenges and open opportunities. Biochim Biophys Acta. 2017;1867:49–57.
6. Schulten HJ, Bangash M, Karim S, Dallol A, Hussein D, Merdad A, Al-Thoubaity FK, Al-Maghrabi J, Jamal A, Al-Ghamdi F. Comprehensive molecular biomarker identification in breast cancer brain metastases. Journal of Translational Medicine. 2017;15:269.

7. Vo JN, Cieslik M, Zhang Y, Shukla S, Xiao L, Zhang Y, Wu YM, Dhanasekaran SM, Engelke CG, Cao X, et al. The Landscape of Circular RNA in Cancer. Cell. 2019;176:869–81 e813.
8. Kristensen LS, Andersen MS, Stagsted LVW, Ebbesen KK, Hansen TB, Kjems J. The biogenesis, biology and characterization of circular RNAs. Nat Rev Genet. 2019;20:675–91.
9. Chen S, Zhao Y. Circular RNAs: Characteristics, function, and role in human cancer. Histol Histopathol. 2018:11969.
10. Li X, Yang L, Chen L-L. The Biogenesis, Functions, and Challenges of Circular RNAs. Molecular cell. 2018;71:428–42.
11. Yu J, Xu QG, Wang ZG, Yang Y, Zhang L, Ma JZ, Sun SH, Yang F, Zhou WP. Circular RNA cSMARCA5 inhibits growth and metastasis in hepatocellular carcinoma. J Hepatol. 2018;68:1214–27.
12. Hu ZQ, Zhou SL, Li J, Zhou ZJ, Wang PC, Xin HY, Mao L, Luo CB, Yu SY, Huang XW, et al. Circular RNA Sequencing Identifies CircASAP1 as a Key Regulator in Hepatocellular Carcinoma Metastasis. Hepatology. 2019.
13. Ding L, Zhao Y, Dang S, Wang Y, Li X, Yu X, Li Z, Wei J, Liu M, Li G. Circular RNA circ-DONSON facilitates gastric cancer growth and invasion via NURF complex dependent activation of transcription factor SOX4. Mol Cancer. 2019;18:45.
14. Zhao W, Cui Y, Liu L, Qi X, Liu J, Ma S, Hu X, Zhang Z, Wang Y, Li H, et al. Splicing factor derived circular RNA circUHRF1 accelerates oral squamous cell carcinoma tumorigenesis via feedback loop. Cell Death Differ. 2020;27:919–33.
15. Zhou J, Zhang S, Chen Z, He Z, Xu Y, Li Z. CircRNA-ENO1 promoted glycolysis and tumor progression in lung adenocarcinoma through upregulating its host gene ENO1. Cell Death Dis. 2019;10:885.
16. Yang H, Li X, Meng Q, Sun H, Wu S, Hu W, Liu G, Li X, Yang Y, Chen R. CircPTK2 (hsa_circ_0005273) as a novel therapeutic target for metastatic colorectal cancer. Mol Cancer. 2020;19:13.
17. Fu B, Zhang A, Li M, Pan L, Tang W, An M, Liu W, Zhang J. Circular RNA profile of breast cancer brain metastasis: identification of potential biomarkers and therapeutic targets. Epigenomics. 2018;10:1619–30.
18. Li K, Guo Q, Zhang X, Dong X, Liu W, Zhang A, Li Y, Yan J, Jia G, Zheng Z, et al. Oral cancer-associated tertiary lymphoid structures: gene expression profile and prognostic value. Clin Exp Immunol. 2020;199:172–81.
19. Han B, Zhang Y, Zhang Y, Bai Y, Chen X, Huang R, Wu F, Leng S, Chao J, Zhang JH, et al. Novel insight into circular RNA HECTD1 in astrocyte activation via autophagy by targeting MIR142-TIPARP: implications for cerebral ischemic stroke. Autophagy. 2018:1–21.
20. Fu B, Long W, Zhang Y, Zhang A, Miao F, Shen Y, Pan N, Gan G, Nie F, He Y, et al. Enhanced antitumor effects of the BRBP1 compound peptide BRBP1-TAT-KLA on human brain metastatic breast cancer. Sci Rep. 2015;5:8029.
21. Wang J, Li S, Li X, Li B, Li Y, Xia K, Yang Y, Aman S, Wang M, Wu H. Circadian protein BMAL1 promotes breast cancer cell invasion and metastasis by up-regulating matrix metalloproteinase9 expression. Cancer Cell Int. 2019;19:182.

22. Conrad C, Götte M, Schlomann U, Roessler M, Pagenstecher A, Anderson P, Preston J, Pruessmeyer J, Ludwig A, Li R, et al. ADAM8 expression in breast cancer derived brain metastases: Functional implications on MMP-9 expression and transendothelial migration in breast cancer cells. Int J Cancer. 2018;142:779–91.
23. Stark AM, Anuszkiewicz B, Mentlein R, Yoneda T, Mehdorn HM, Held-Feindt J. Differential expression of matrix metalloproteinases in brain- and bone-seeking clones of metastatic MDA-MB-231 breast cancer cells. J Neurooncol. 2007;81:39–48.
24. Xing F, Sharma S, Liu Y, Mo YY, Wu K, Zhang YY, Pochampally R, Martinez LA, Lo HW, Watabe K. miR-509 suppresses brain metastasis of breast cancer cells by modulating RhoC and TNF-α. Oncogene. 2015;34:4890–900.
25. Wang YH, Sui XM, Sui YN, Zhu QW, Yan K, Wang LS, Wang F, Zhou JH. BRD4 induces cell migration and invasion in HCC cells through MMP-2 and MMP-9 activation mediated by the Sonic hedgehog signaling pathway. Oncol Lett. 2015;10:2227–32.
26. Fan L, Cao Q, Liu J, Zhang J, Li B. Circular RNA profiling and its potential for esophageal squamous cell cancer diagnosis and prognosis. Mol Cancer. 2019;18:16.
27. Liu J, Li D, Luo H, Zhu X. Circular RNAs: The star molecules in cancer. Mol Aspects Med. 2019;70:141–52.
28. Arnaiz E, Sole C, Manterola L, Iparraguirre L, Otaegui D, Lawrie CH. CircRNAs and cancer: Biomarkers and master regulators. Semin Cancer Biol. 2019;58:90–9.
29. Lei B, Tian Z, Fan W, Ni B. Circular RNA: a novel biomarker and therapeutic target for human cancers. Int J Med Sci. 2019;16:292–301.
30. Kristensen LS, Hansen TB, Venø MT, Kjems J. Circular RNAs in cancer: opportunities and challenges in the field. Oncogene. 2018;37:555–65.
31. Huang R, Zhang Y, Han B, Bai Y, Zhou R, Gan G, Chao J, Hu G, Yao H. Circular RNA HIPK2 regulates astrocyte activation via cooperation of autophagy and ER stress by targeting MIR124–2HG. Autophagy. 2017;13:1722–41.
32. Bach DH, Lee SK, Sood AK. Circular RNAs in Cancer. Mol Ther Nucleic Acids. 2019;16:118–29.
33. Liu H, Hu G, Wang Z, Liu Q, Zhang J, Chen Y, Huang Y, Xue W, Xu Y, Zhai W. circPTCH1 promotes invasion and metastasis in renal cell carcinoma via regulating miR-485-5p/MMP14 axis. Theranostics. 2020;10:10791–807.
34. Xu Y, Yu J, Huang Z, Fu B, Tao Y, Qi X, Mou Y, Hu Y, Wang Y, Cao Y, et al. Circular RNA hsa_circ_0000326 acts as a miR-338-3p sponge to facilitate lung adenocarcinoma progression. J Exp Clin Cancer Res. 2020;39:57.
35. Liu J, Zhang X, Yan M, Li H. Emerging Role of Circular RNAs in Cancer. Front Oncol. 2020;10:663.
36. Wang X, He Y, Mackowiak B, Gao B. MicroRNAs as regulators, biomarkers and therapeutic targets in liver diseases. Gut. 2020:gutjnl-2020-322526.

37. Huang H, Huang J, Yao J, Li N, Yang Z. miR-125a regulates HAS1 and inhibits the proliferation, invasion and metastasis by targeting STAT3 in non–small cell lung cancer cells. J Cell Biochem. 2020;121:3197–207.
38. Xiong J, Tu Y, Feng Z, Li D, Yang Z, Huang Q, Li Z, Cao Y, Jie Z. Epigenetics mechanisms mediate the miR-125a/BRMS1 axis to regulate invasion and metastasis in gastric cancer. OncoTargets Therapy. 2019;12:7513–25.
39. Zhang Y, Zhang D, Lv J, Wang S, Zhang Q. MiR-125a-5p suppresses bladder cancer progression through targeting FUT4. Biomed Pharmacother. 2018;108:1039–47.
40. Yamamoto T, Hirosue A, Nakamoto M, Yoshida R, Sakata J, Matsuoka Y, Kawahara K, Nagao Y, Nagata M, Takahashi N, et al. BRD4 promotes metastatic potential in oral squamous cell carcinoma through the epigenetic regulation of the MMP2 gene. Br J Cancer. 2020;123:580–90.
41. Wang Y, Lin Q, Song C, Ma R, Li X. Circ_0007841 promotes the progression of multiple myeloma through targeting miR-338-3p/BRD4 signaling cascade. Cancer Cell Int. 2020;20:383.

Figures

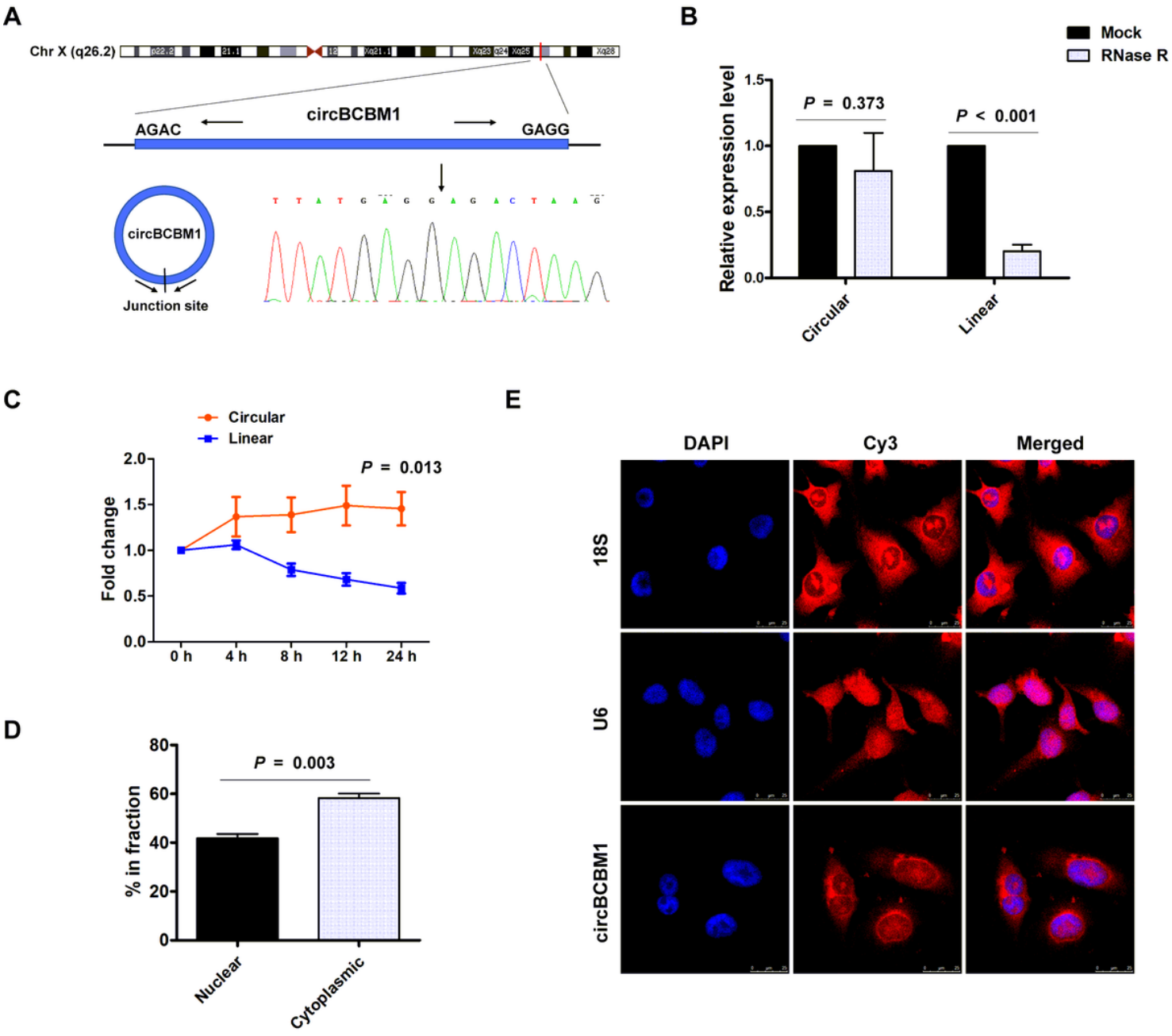

Figure 1

Characterization of circBCBM1 in 231-BR cells. (A) The schematic diagram of genomic location and splicing pattern of circBCBM1. The splice junction was verified by Sanger sequencing. (B) RT-qPCR analysis for the abundance of circBCBM1 and its linear counterpart after treatment with RNase R in 231-BR cells. The amount of circBCBM1 and its linear counterpart were normalized to the value measured in the mock treatment. (C) The expression level of circBCBM1 and its linear counterpart after treatment with Actinomycin D (2.5 μg/ml) at the indicated time points in 231-BR cells. (D) Cellular RNA fractionation analysis. CircBCBM1 was mainly located in the cytoplasm of 231-BR cells. (E) RNA fluorescence in situ hybridization (FISH) for circBCBM1. Nuclei were stained with 4,6-diamidino-2-phenylindole (DAPI). Scale bar, 25 μm. Data are presented as means ± SEM (B-D).

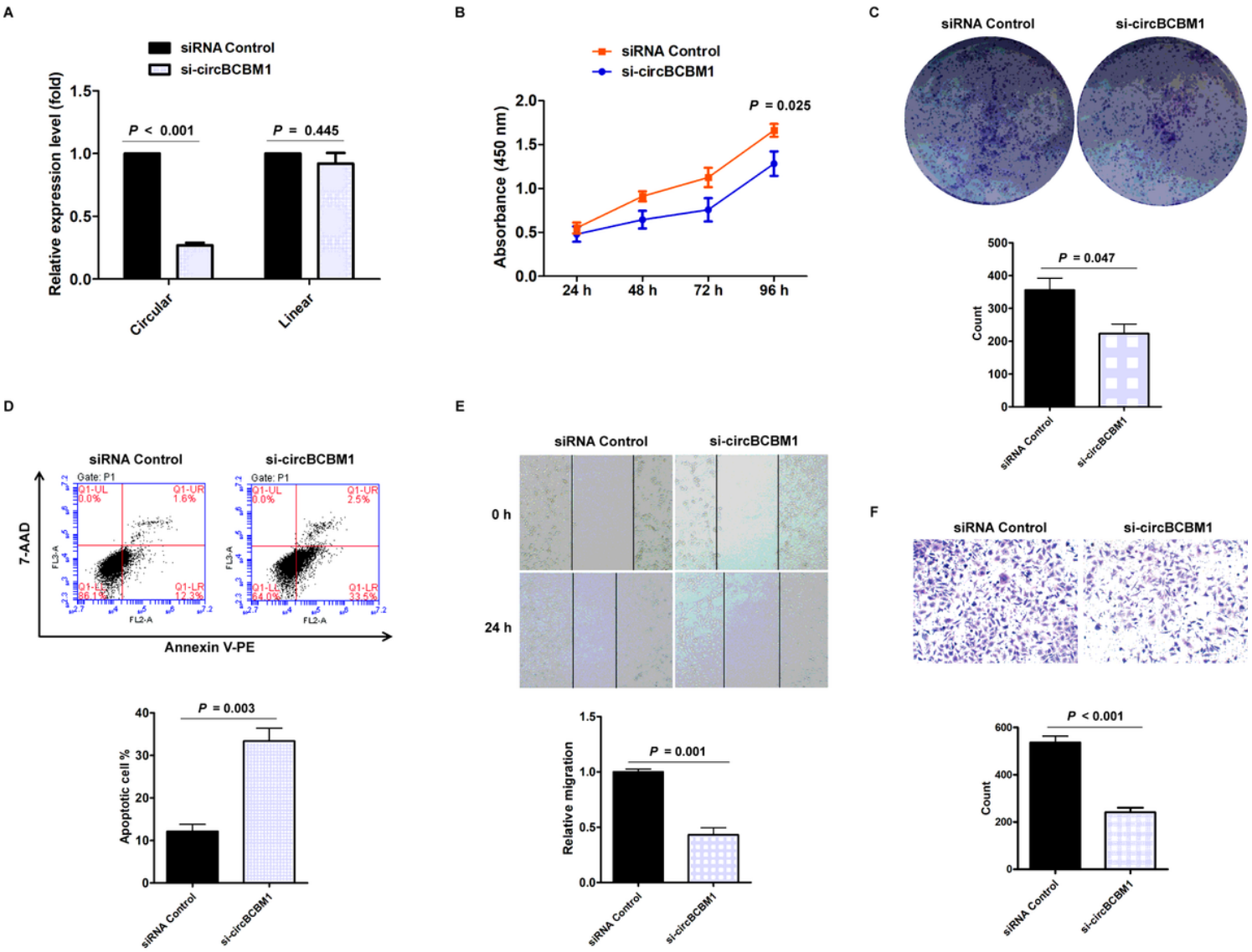

Figure 2

Silencing of circBCBM1 inhibits proliferation and migration and induces apoptosis of 231-BR cells in vitro. 231-BR cells were either transfected with si-circBCBM1 or siRNA Control. (A) RT-qPCR for the expression analysis of circBCBM1 and its linear counterpart. The relative expression levels were normalized to the values in the siRNA-control group. (B) CCK-8 assay. (C) Colony formation assay. (D) Annexin V-PE/ 7-AAD staining and FACS quantified the apoptotic cells percentage. (E) Wound-healing assay. (F) Transwell migration assay. Data are presented as means ± SEM (A-F). si-circBCBM1, siRNA against circBCBM1; siRNA Control, siRNA for negative control.

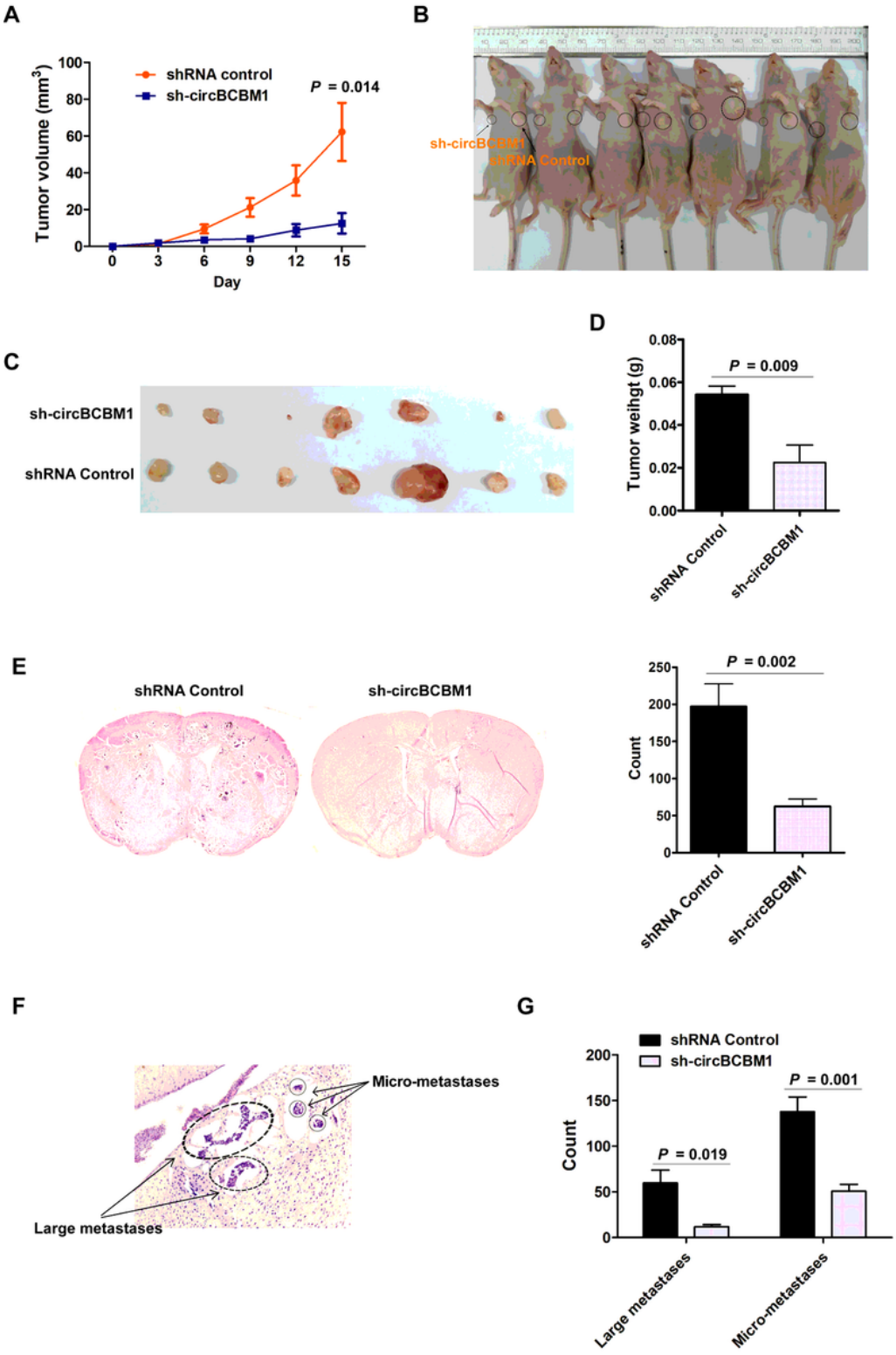

Figure 3

Silencing of circBCBM1 inhibits growth and brain metastasis of 231-BR cells in vivo. Nude mice were subcutaneously injected 231-BR cells with stable transfection of negative control (shRNA Control) or shRNA-circBCBM1 (n = 7) (A-D). (A) Tumor growth curves of subcutaneous models. (B) Images of the subcutaneous xenograft models on the 15th day. (C) Images of the dissected subcutaneous tumors. (D) Weights of the dissected subcutaneous tumors. Brain metastasis model was generated by injection of

231-BR cells with stable transfection of negative control (shRNA Control) or shRNA-circBCBM1 into the left cardiac ventricle of mouse heart. After 4 weeks, the brains were collected and metastatic nodules were counted after H&E staining (n = 6) (E-G). (E) Representative H&E images and quantification of brain metastases. (F) H&E staining of the brain sections showed large metastases (ovals) and micro-metastases (circles). (G) Quantification of the counts of large metastases and micro-metastases. Data are presented as means ± SEM (A, D, E and G).

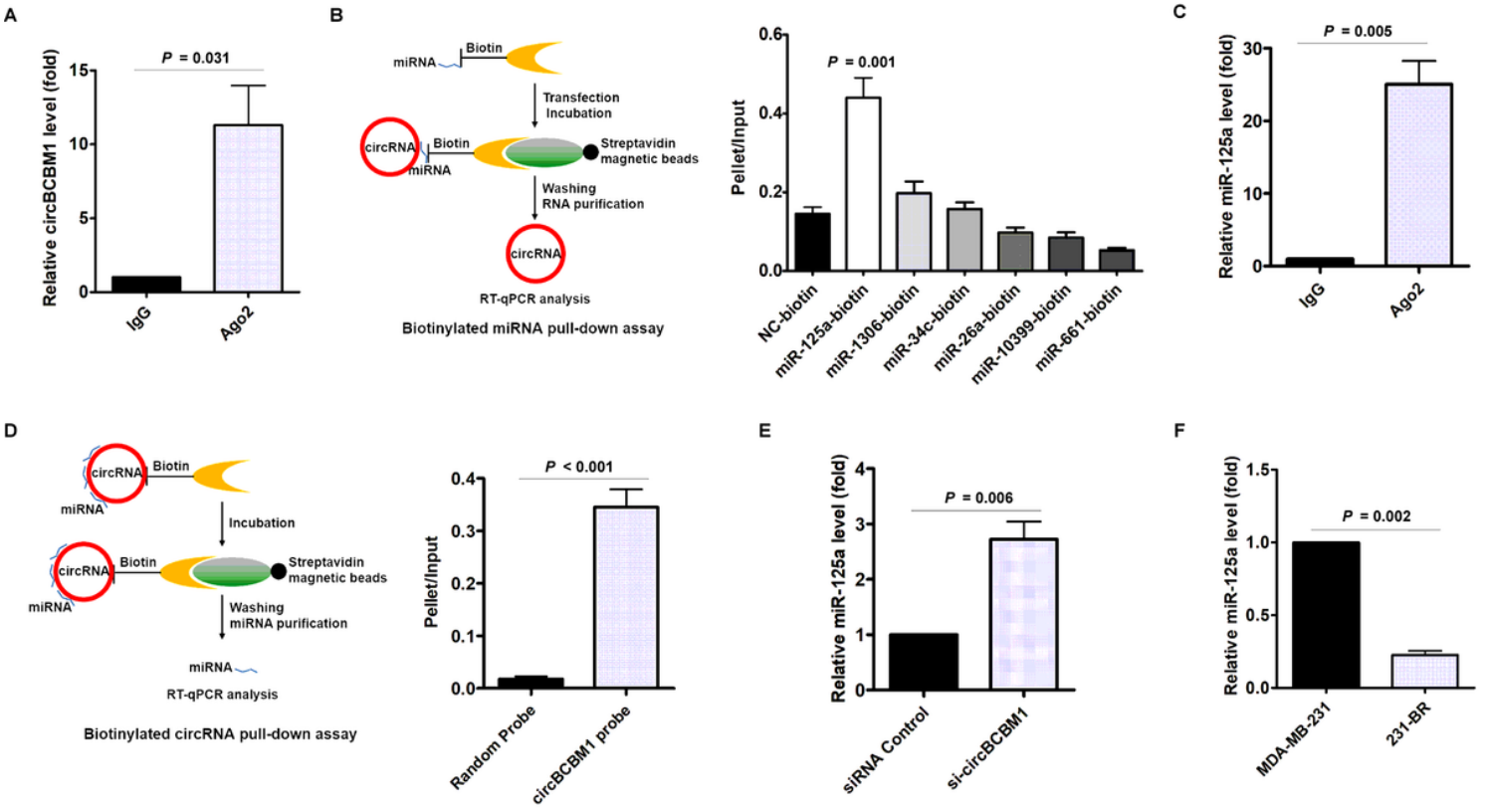

Figure 4

CircBCBM1 directly interacts with miR-125a in 231-BR cells. (A) RNA immunoprecipitation (RIP) and RT-qPCR assays were conducted to analyze the binding of circBCBM1 to Ago2 protein. (B) Biotinylated miRNA pull-down assay. RNA was affinity-isolated by biotinylated miR-125a, miR-1306, miR-34c, miR-26a, miR-10399, miR-661 or the negtive control miRNA, and the circBCBM1 and GAPDH mRNA levels were quantified by RT-qPCR. Relative level of circBCBM1 was normalized to input. (C) RIP and RT-qPCR assays were performed to analyze the binding of miR-125a to Ago2 protein. (D) Biotinylated circBCBM1 pull-down assay. RNA was affinity-isolated by biotinylated circBCBM1 or the control probe, and the circBCBM1 and U6 levels were analyzed by RT-qPCR. Relative level of miR-125a was normalized to input. (E) RT-qPCR analysis of miR-125a level in 231-BR cells transfected with si-circBCBM1 or siRNA-control. (F) The relative level of miR-125a in 231-BR cells versus the parental MDA-MB-231 cells. Data are presented as means ± SEM (A-F).

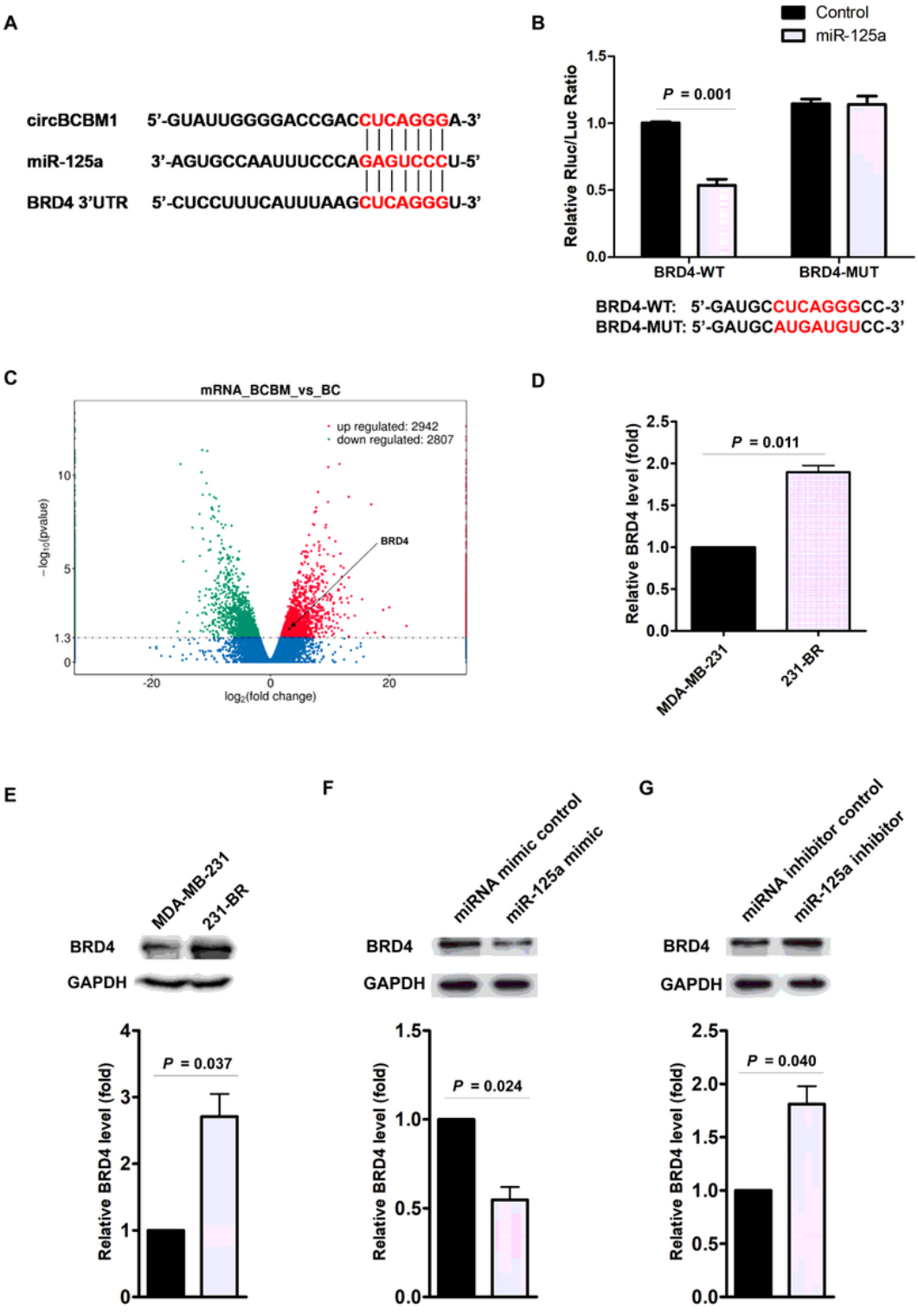

Figure 5

BRD4 is the downstream target of the circBCBM1/miR-125a axis. (A) Putative miR-125a binding site in BRD4. The potential complementary residues are shown in red. (B) Relative luciferase activity of BRD4 wild-type (BRD4-WT) and 3′-UTR mutant (BRD4-MUT) constructs cotransfected with miR-125a mimics or miRNA negative control. (C) Volcano plots assessing the differentially expressed mRNAs between 231-BR (BCBM) and its parental MDA-MB-231 cell (BC) groups. (D and E) RT-qPCR (D) and western blot (E)

analyses of BRD4 expression in 231-BR cells versus the parental MDA-MB-231 cells. (F and G) Western blot assays examined the expression levels of BRD4 in 231-BR cells transduced with miR-125a mimics (F) or miR-125a inhibitors (G). miRNA mimic control (F) and miRNA inhibitor control (G) were used as the miRNA mimic and inhibitor negative control, respectively. Data are presented as means ± SEM (B, D-G).

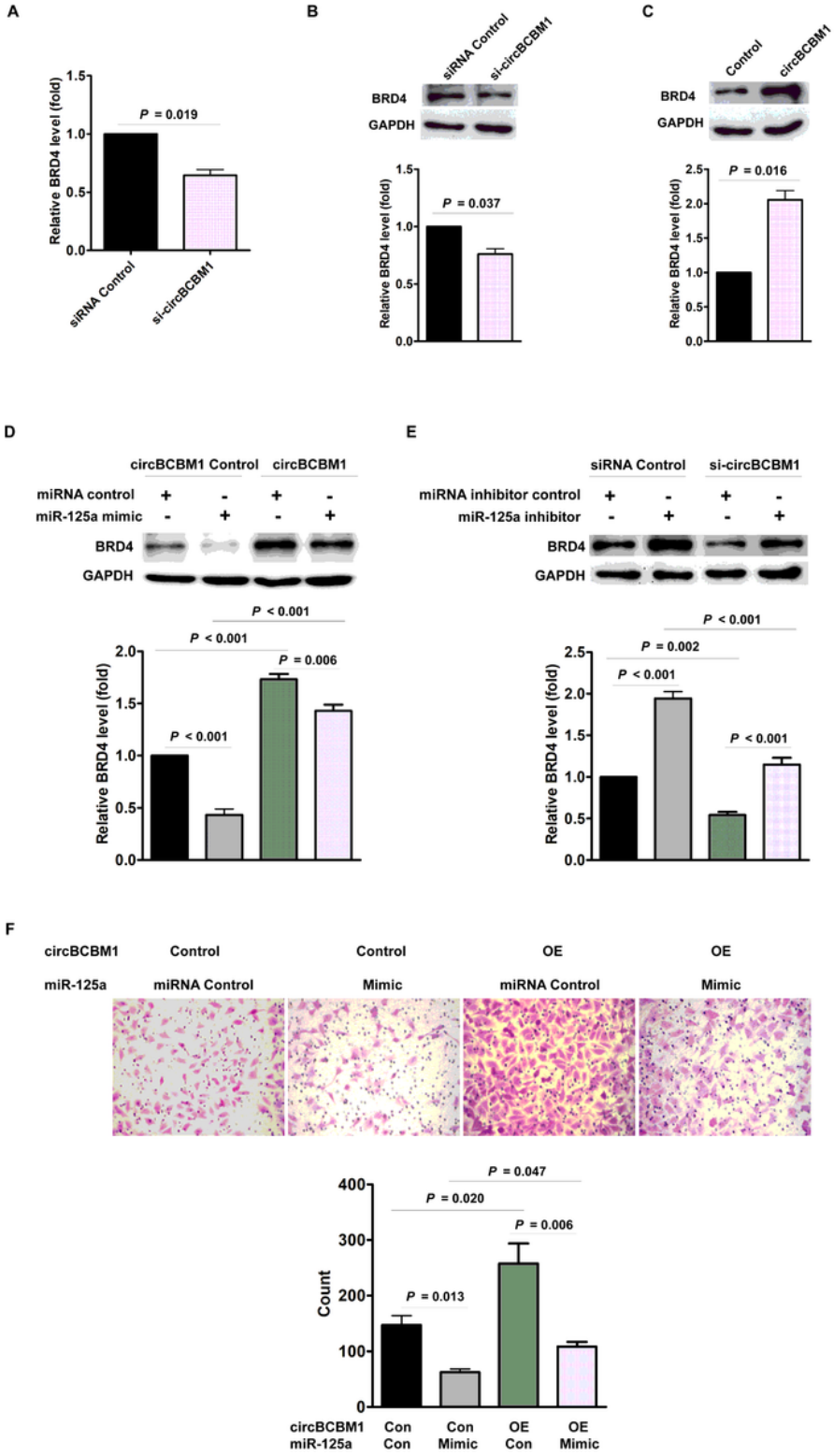

Figure 6

CircBCBM1 promotes cell migration via circBCBM1/miR-125a/BRD4 axis in 231-BR cells. (A and B) RT-qPCR (A) and western blot (B) assays analyzed the expression of BRD4 in 231-BR cells after treatment with si-circBCBM1. (C) Western blot analysis of BRD4 expression in 231-BR cells transfected with control vector (Control group) or circBCBM1 over-expression plasmid (circBCBM1 group). (D) Transduction of 231-BR cells with circBCBM1 overexpressing lentivirus significantly increased miR-125a-inhibited BRD4 expression as determined by western blot analysis. (E) Transduction of 231-BR cells with circBCBM1 siRNA significantly inhibited miR-125a inhibitor induced BRD4 expression as determined by western blot analysis. (F) Overexpression of circBCBM1 rescued the migration of 231-BR cells after transfection with miR-125a mimics as determined by transwell migration assay. OE: overexpression; Con: control. Data are presented as means ± SEM (A-F).

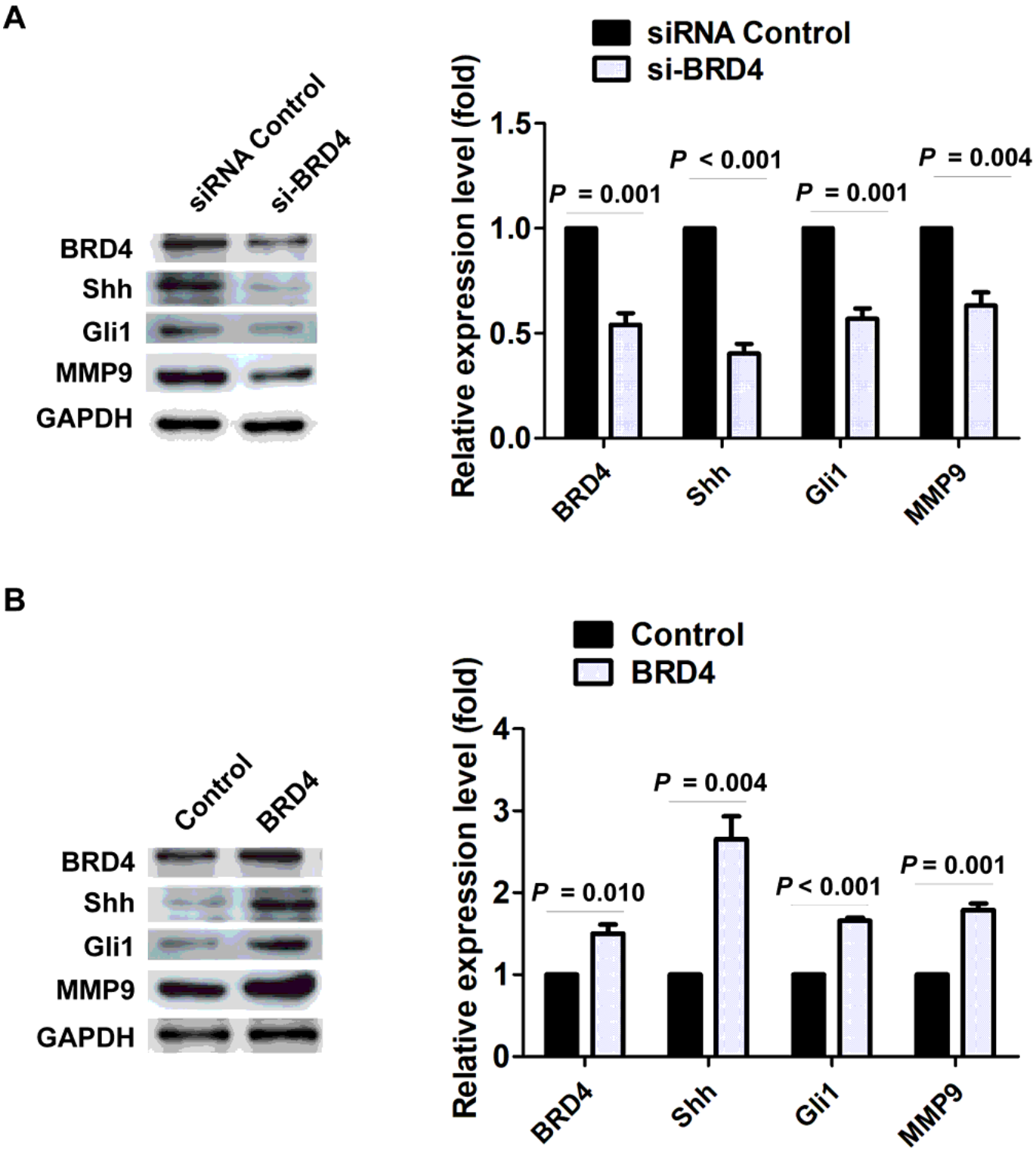

Figure 7

BRD4 promotes MMP9 expression through SHH signaling pathway in 231-BR cells. (A and B) Western blot analyses of BRD4, Shh, Gli and MMP9 expression in 231-BR cells transfected with si-BRD4 (A) or BRD4 over-expression plasmid (BRD4 group) (B). The relative expression level was normalized to that of the siRNA control group (A) or control vector group (B). Data are presented as means ± SEM.

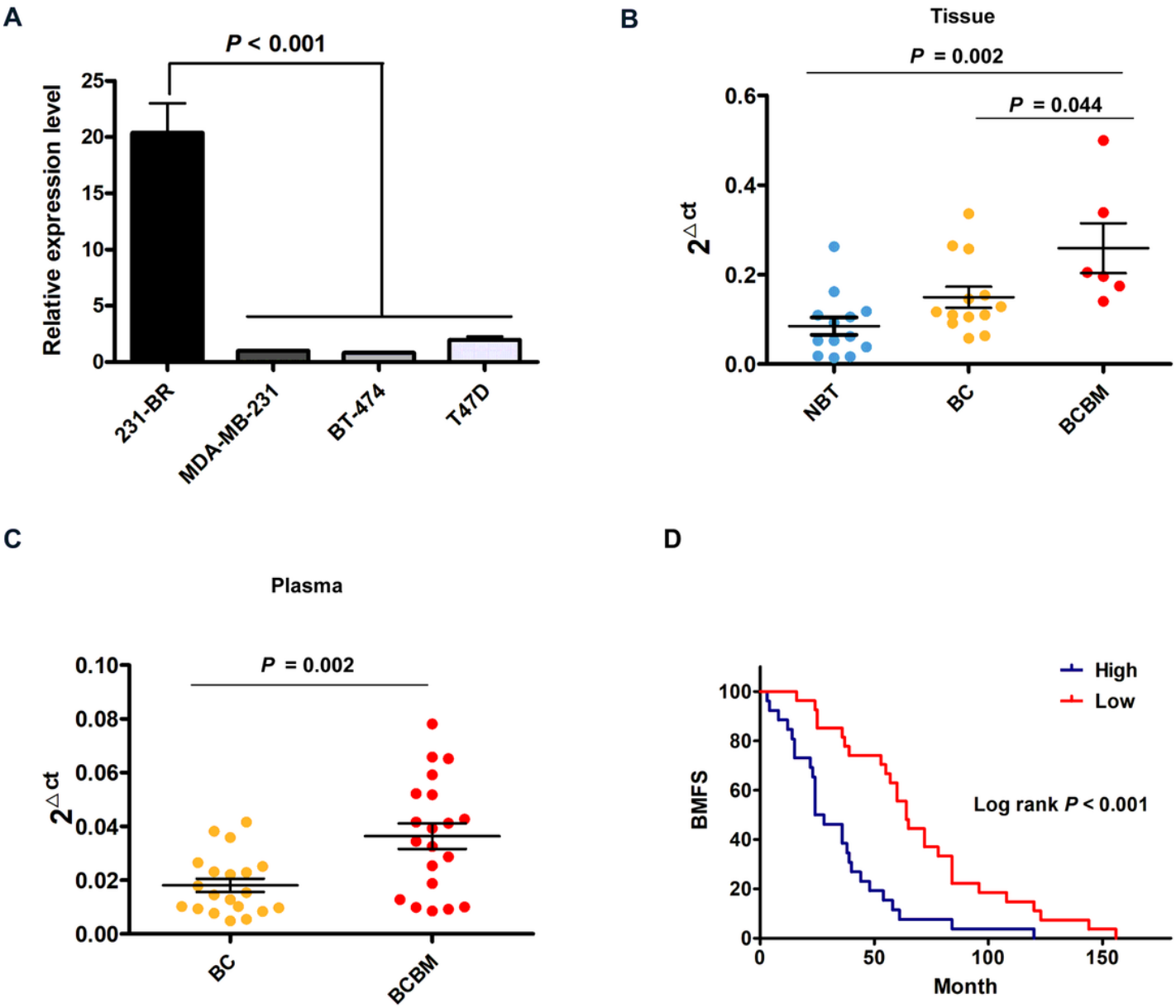

Figure 8

The potential diagnostic and prognostic value of circBCBM1. (A) RT-qPCR analysis of circBCBM1 expression in 231-BR cells versus other breast cancer cells (MDA-MB-231, BT-474 and T47D). The relative expression level was normalized to that of MDA-MB-231 cells. (B and C) RT-qPCR analyses of circBCBM1 expression level in tissue (B) and plasma (C) samples. For (B), NBT, adjacent normal breast tissues, n = 13; BC, breast cancer tissues, n = 13; BCBM, breast cancer brain metastasis tissues, n = 6. For (C), BC, breast cancer plasmas, n = 20; BCBM, breast cancer brain metastasis plasmas, n = 20. Data are presented as means ± SEM (A-C). (D) Kaplan-Meier analysis for brain metastasis-free survival (BMFS) of 53 BCBM patients. Patients were divided into two groups on the basis of the expression of circBCBM1 in the patients' primary tumors. P value was calculated using log-rank test.

Supplementary Files

This is a list of supplementary files associated with this preprint. Click to download.

- SupplementaryFiles.docx